Journal of Archaeological Science: Reports 53 (2024) 104402

Contents lists available at ScienceDirect

Journal of Archaeological Science: Reports

journal homepage: www.elsevier.com/locate/jasrep

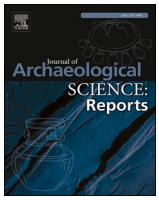

The ceramics from Empúries county (Catalonia) in the 10th-11th centuries AD. An archaeometric approach☆

Marta Valls Llorens [a,*], Jaume Buxeda i Garrigós [a], Marisol Madrid i Fernández [a], Roberta Bruna Mentesana [a], Anna Maria Puig Griessenberger [b]

[a] Cultura Material i Arqueometria UB (ARQUB, GRACPE), Departament d'Història i Arqueologia, Universitat de Barcelona, C/ de Montalegre, 6, 08001 Barcelona, Catalonia, Spain
[b] Institut d'Estudis Empordanesos, Avinguda dels Pirineus 19, escala B-4, 17600 Figueres, Catalonia, Spain

ARTICLE INFO

Keywords:
Provenance
Technology
XRF
XRD
SEM
Petrography
Catalan Counties

ABSTRACT

The sixty ceramic individuals studied in this project were recovered in Empúries county, including a few ceramics from Besalú and Rosselló counties (Catalonia) for comparison. These ceramics, dated to the 10th—11th centuries AD, belong to a historical period related to the creation and consolidation of the Catalan Counties. This period is poorly studied from an archaeological point of view, so there is little information about ceramic production and distribution, which this research aims to change by identifying the provenance and some elements of the manufacturing techniques. For this purpose, the ceramic sherds have been chemically and mineralogically characterised by X-ray fluorescence (XRF) and X-ray diffraction (XRD), respectively. Their microstructure and sintering state have been determined by scanning electron microscopy coupled to energy-dispersive X-ray spectroscopy (SEM), and petrographic analyses have been performed, too. Results confirm distribution patterns and the evidence of similar technical traditions in different Counties. Finally, the contrast with the database enables us to relate some of the individuals analysed in this study to some others from the area of the County of Empúries dating from the Visigoth period (7th—8th centuries) in line with their exceptionally high concentrations of Na_2O.

1. Introduction and objectives

The Islamic occupation of the Iberian Peninsula started in AD 711. During the 8th century, a fast expansion took place, creating the Islamic territory of Al-Andalus, which extended by almost all of the Iberian Peninsula and some areas of the Southeast of current France. In 732, the Carolingian army defeated the Islamic troops at the Battle of Tours (or Poitiers), which led to a fast retreat to the area of the Pyrenees. Since the 9th century, following the Carolingian expansion, several Christian counties were created in the area of current Catalonia (Ribagorça, Pallars, Urgell, Cerdanya, Osona, Girona, Barcelona, Besalú, Empúries and Rosselló). Nevertheless, the different counties' territory would undergo modifications until 1402, when all the counties would form part of the domain of the Count of Barcelona (Abadal 1950).

These Catalan Counties were, at first, politically dependent on the Carolingian monarchs. Nevertheless, they started to establish some degree of independence after the refusal of Carolingian king Lothair of France to help the Catalan territories against the looting of Barcelona by the Islamic military leader al-Mansur in 985. Consequently, in 988, Count Borrell II of Barcelona refused to renew his vassalage pact with King Hug Capet of France, the first king of the Capetian dynasty after the extinction of the Carolingian one. This independence process with respect to the monarchs of France was legally completed in 1258 with the Treaty of Corbeil (Feliu i Montfort, 2007; Cingolani, 2010), but from 1162 onwards, the Count of Barcelona was already also the King of Aragon, even if the County of Barcelona and the Kingdom of Aragon were separate entities under the same ruler, forming the Crown of Aragon.

This study focuses on characterising a ceramic set recovered in several archaeological sites in the County of Empúries, with a few ceramics from the counties of Rosselló and Besalú for comparison (Fig. 1). These ceramics are dated between the 10th and the 11th centuries,

☆ Not standard abbreviations used in this article, corresponding to archaeological sites: CDE (Castelló d'Empúries), EMP (Sant Martí d'Empúries), SCR (Santa Creu de Rodes), TLB (Torre Lardera), VIL (Vilarnau), CDR (Camp del Rei), PGR (Puig-Rom).

* Corresponding author.
E-mail address: mvalls@ub.edu (M. Valls Llorens).

https://doi.org/10.1016/j.jasrep.2024.104402
Received 22 October 2023; Received in revised form 18 December 2023; Accepted 17 January 2024
Available online 31 January 2024

according to stratigraphy and typological analysis. That is, between the last decades of the Carolingian domain of the Catalan Counties and the first steps through their *de facto* independence. Despite being a moment of political instability and change, the study of the material culture associated with this period has deserved little attention from scholars (Abadal 1961; Bonnassie 1979; Passarrius,Donat and Catafau, 2008; Puig Griessenberger, 1996; Rendu, 2003; Salrach, 1993).

Regarding the archaeological contexts from the County of Empúries, Sant Martí d'Empúries (from now onwards, EMP) (42°08′24″ N, 3°07′04″ E) was the first capital of this County since its creation at the beginning of the 9th century. The recovered samples were in a *silo* (dug structure used to store grains) dating back to the 8th-11th centuries (Aquilué and Burés, 1999: 423-426). This town suffered several maritime attacks during the 10th century, and the capital was transferred to Castelló d'Empúries (CDE) (42°15′35″ N, 3°04′24″ E) in the 11th century, from where most of the studied individuals came. The ceramics recovered in CDE belong to the preparation of the ground for building the Romanesque Basilica of Santa Maria (1064) and date from the 10th-11th centuries (Bolòs and Hurtado, 1998, 36; Puig 2018, 6). Finally, the Santa Creu de Rodes (SCR) settlement (42°19′34″ N, 3°09′39″ E) is the last one of the contexts sampled in the County of Empúries. This site was founded at some point in the 9th-10th centuries. The site has a pre-Romanesque church, a small necropolis, and some houses, and will last until the 15th century (Ollich, 1999). The ceramics analysed have been dated to the 11th century and belong to the archaeological layers covering the necropolis; after this phase, some houses were built over (Ollich et al., 2018).

For comparison, we have considered two ceramics from the archaeological site of Torre Lardera (TLB) (42°12′00″ N, 2°41′36″ E) in Besalú—the capital of the County of Besalú—, one of the towers that would be part of the medieval city walls. The ceramics were found in some *silos* in layers dating back to the end of the 10th century (Frigola, 2011; Valenzuela,Madroñal and Frigola, 2013; Frigola,Madroñal and Valenzuela, 2014). Moreover, two archaeological sites have been considered for the northern County of Rosselló, north of the Albera range, which makes up the Eastern area of the Pyrenees. On the one hand, Camp del Rei (CDR) (42°44′49″ N, 2°48′24″ E) is in the town of Baixàs, a settlement founded during the Carolingian occupation of this area. Up to now, CDR is the most representative archaeological site studied in Rosselló for the Early Medieval times, as it has the highest number of structures and materials identified for this phase. The ceramics recovered here correspond to the 10th-11th centuries, and they were found in a *silo* located in a storage area of the settlement (Passarrius and Catafau 2001, 109-132; Passarrius,Donat and Catafau, 2008, 48).

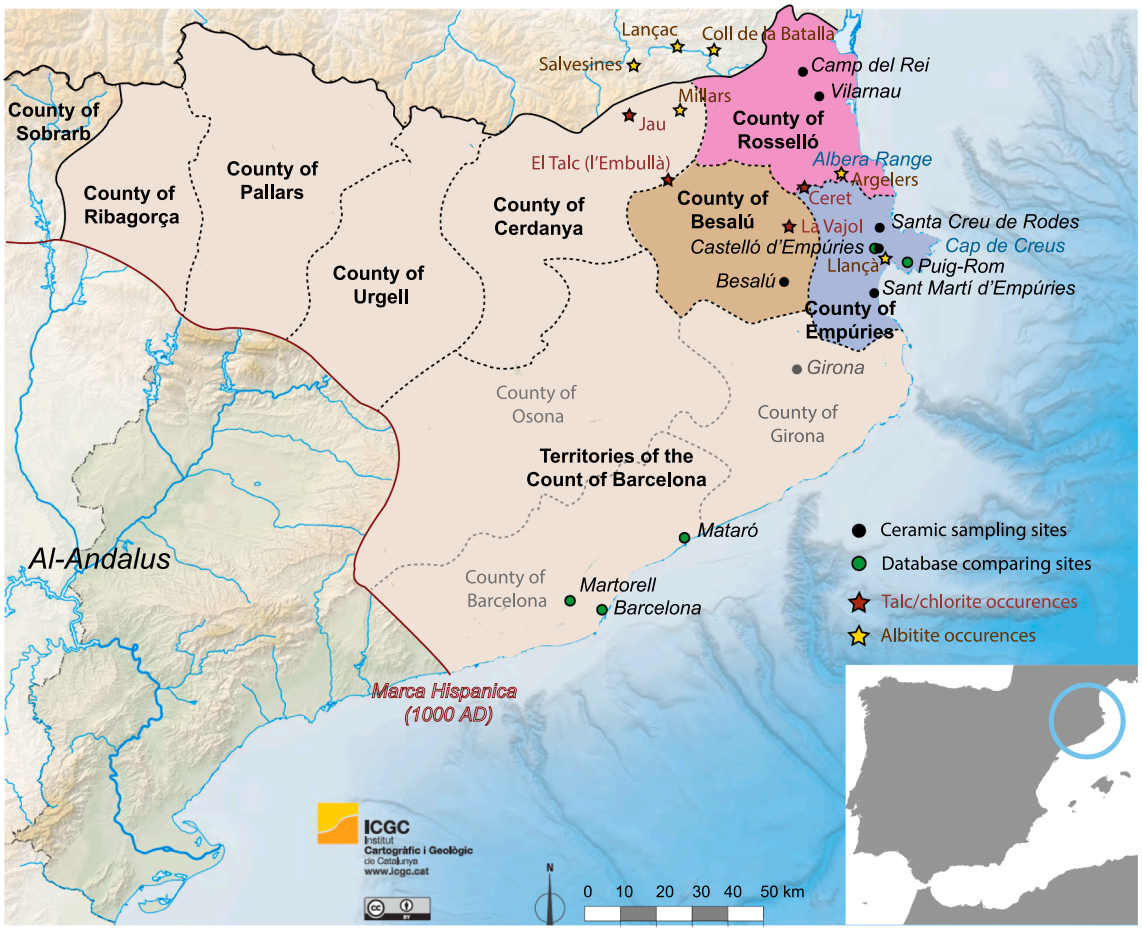

Fig. 1. Location of the sampled sites. Black dots: archaeological sites sampled for this project; Green dots: archaeological sites related to the sampled ceramics. The following acronyms for archaeological sites will be used along the paper: CDE, Castelló d'Empúries; EMP: Sant Martí d'Empúries; SCR: Santa Creu de Rodes; TLB: Besalú; PGR: Puig-Rom; CDR: Camp del Rei; VIL: Vilarnau. (For interpretation of the references to colour in this figure legend, the reader is referred to the web version of this article.)

On the other hand, Vilarnau (VIL) (42°41′43″ N, 2°53′23″ E)[1] is similar to CDR, as they are very close sites corresponding to the same chronology. The ceramics recovered here have been found in a *silo* dating from the 10th-11th centuries (Passarrius, Donat and Catafau 2008, 398-399).

2. Materials and methods

2.1. Materials

This paper contributes to fill in the gap in Medieval studies of material culture by analysing for the first time a considerable number (60) of ceramics recovered in several archaeological sites to understand the provenance and circulation of the analysed ceramics. The sampled ceramics correspond to 34 undetermined fragments—18 with a spatulated surface treatment surface (*i.e.*, a surface smoothed with a stick or *spatula*)—, and 26 sherds that can be classified into cooking ware (9 casseroles and casserole covers, 3 cooking plaques and 8 cooking pots) and coarse ware (1 *sitra* and 5 pitchers). Among the cooking ware, we must highlight the cooking plaques that seem characteristic of early medieval contexts in this area, as they have not been identified in other chronologies or places (Passarrius,Donat and Catafau, 2008, 401 and 439). They are a circular and plain ceramic individual approximately 2 cm thick and 40–50 cm in diameter that should be tentatively used on fire as a cooking device. Concerning coarse ware, we must highlight the presence of a *sitra*, a specific type of pitcher characteristic of the Carolingian material culture, having a spout, a high plain handle and a spatulated surface. *Sitres* seem to have originated in the Rhine Valley and were introduced in Catalonia after the Carolingian conquest (Riu, 1984, 35), becoming the most distinctive element of the Carolingian material culture and lasted until the 11th century. All these ceramics are coarse and handmade. The distribution of the ceramic types analysed among the different archaeological sites is detailed in Table 1 and Table 1 of the Supplementary Material. It must be noted that individuals CDE141 and 142 have been classified as casseroles or cooking pots as they could not be defined because of the size of the sherds. Detailed drawings and photographs of the most representative ceramics can be found in Fig. 8, which illustrates the classification of the ceramics in the significant chemical groups defined.

2.2. Methods

All individuals have been characterised chemically through wavelength dispersive X-ray fluorescence (WD-XRF) and mineralogically through powder X-ray diffraction (PXRD). A subsample of carbon-coated 20 individuals was studied by scanning electron microscopy with energy-dispersive X-ray spectroscopy (SEM-EDX) (Table 1). The petrographic observations were made on 21 individuals using an Olympus BX43P microscope. Fabric description has been made considering the Whitbread's system (Whitbread, 1989,1995,2016), but due to the small number of individuals and the variability encountered, we prefered to summarise the petrographic features in a table (Supplementary Material, Table 2).

A detailed description is in the "Methods and Protocols" document in the Supplementary Material.

3. Results

3.1. Chemical analysis

The results of elemental concentrations determined by WD-XRF (Table 3 of the Supplementary Material) are compositional data that have been alr (additive log-ratio) and clr (centred log-ratio) transformed (Aitchison, 1986; Buxeda i Garrigós, 1999; Egozcue and Pawlowsky-Glahn, 2011; Martín-Fernández et al., 2015; Buxeda i Garrigós, 2018). The statistical data treatment of the chemical data was performed using R (R Core Team 2022). The first analysis carried out was to calculate the variation matrix that completely determines the covariance structure of compositional data and provides the total variation (*tv*) of the analysed ceramic assemblage (Fig. 2) (Aitchison, 1986; Buxeda i Garrigós and Kilikoglou, 2003). The total variation (*tv*) for the overall data set equals 1.2, which indicates a polygenic group. If the total variation quantifies how different the chemical data are, the information entropy, or Shannon index, quantifies how evenly the chemical differences are related to the retained components. The compositional evenness graph reveals that the elements that introduce more variability are CaO, Ni, and Na_2O ($\tau_j < 0.3$, *i.e.*, *tv* accounts for less than 30 % of the trace of the variance–covariance matrix after an alr transformation using any of these elements as a divisor), and, to a lesser extent, V, Cr, Sr, Ba, and MnO ($0.3 < \tau_j < 0.5$). All these indicators show that even if the chemical variability is linked to a few elements, the composition varies significantly in all retained components (the information entropy has a value of 3.7 Sh, *i.e.*, 81.69 % of the maximum attainable), meaning that many elements are introducing significant variability in the analysis. Regarding CaO, the variability is probably due to the composition of individual CDE151 (CaO = 4.11 %), which exhibits a significantly higher CaO concentration than the rest of the individuals analysed (Table 3 of the Supplementary Material).

As a summary of all the exploratory data analysis, a dendrogram was obtained from the cluster analysis performed on the 60 individuals studied using the square Euclidean distance and the centroid agglomerative algorithm on the clr transformed subcomposition Na_2O, MgO, Al_2O_3, SiO_2, K_2O, CaO, TiO_2, V, Cr, MnO, Fe_2O_3, Ni, Zn, Sr, Ce, Zr, Nb, and Ba. This graph showed a structure divided into five chemical groups plus seventeen ungrouped individuals, from which individual CDE151 significantly differs. To further investigate these groups, as well as the still ungrouped individuals, we compared these results with 194 individuals from the ARQUB research unit database, chronologically or geographically close to the contexts studied: (i) a possible ceramic production from CDE dating from the 15th—16th centuries (Buxeda i Garrigós and Madrid i Fernández, 2016b); (ii) one individual from the archaeological site of Ruscino (42°41′43″ N, 2°53′23″ E) and seven Visigoth ceramics recovered in the fortress placed in Cap de Creus of Puig-Rom (Roses, County of Empúries) (42°15′06″ N, 3°11′13″ E), and dating from the 7th—8th centuries (Buxeda i Garrigós et al., 2018, Subías Pascual et al., 2016, 2020); some ceramic individuals recovered in (iii) the plaça del Rei, (iv) Saló del Tinell, (v) and Pedralbes ceramic kiln (Barcelona, County of Barcelona) (41°23′35″ N, 2°10′10″ E), corresponding to different archaeological contexts between the 6th and the 8th centuries (Beltrán de Heredia et al., 2018; Buxeda i Garrigós and Cau Ontiveros, 2005, 2006); and (vi) a set of materials recovered in Mataró (County of Barcelona) (41°32′21″ N, 2°26′15″ E) (Buxeda i Garrigós and Cau Ontiveros, 2004) and (vii) Santa Maria de Martorell (County of Barcelona) (41°28′36″ N, 1°53′14″ E)[2] (Buxeda i Garrigós and Madrid i Fernández, 2009), both corresponding to the 6th—7th centuries.

The only similar connection that could be established was between 2 of our individuals (CDE149 and 151, two loners) and the 5 low calcareous ceramics from the Visigoth fortress of Puig-Rom (from now onwards PGR) (Fig. 1), which form the chemical group CGPGR01. The dendrogram of our ceramics together with these 5 Visigoth ones (Fig. 3),

[1] The position given for Sant Martí d'Empúries, Castelló d'Empúries, Santa Creu de Rodes, Torre Lardera, Camp del Rei and Vilarnau archaeological sites corresponds to the modern towns of Sant Martí d'Empúries, Castelló d'Empúries, Port de la Selva, Besalú, Baixàs and Perpinyà, respectively.

[2] The position given for Castelló d'Empúries, Ruscino, Puig-Rom, Mataró and Santa Maria de Martorell archaeological sites corresponds to the modern towns and cities of Castelló d'Empúries, Perpinyà, Roses, Mataró and Martorell, respectively. The position given for Plaça del Rei, Saló del Tinell and Pedralbes archaeological sites corresponds to the city of Barcelona.

Table 1
Studied individuals by site and ceramic class; *: individuals classified as casseroles that might be cooking pots; PE: petrographic examination; SEM: SEM examination.

	Sitra	Pitcher	Casserole and casserole cover	Cooking plaque	Cooking pot	Spatulated sherds	Coarse ware sherds	Total
Sant Martí d'Empúries (EMP)	(1) EMP502	(0)	(1) EMP503$^{PE, SEM}$	(0)	(0)	(1) EMP501$^{PE, SEM}$	(0)	**3**
Castelló d'Empúries (CDE)	(0)	(5) CDE147, 150, 152, 153, 155	(8) CDE136, 138, 141*, 142*, 144, 148, 149^{PE}, 154	(2) CDE101$^{PE, SEM}$, 112^{PE}	(6) CDE137, 139, 140, 145, 146, 151^{PE}	(12) CDE108, 111, 113, 115^{PE}, 120, 122^{PE}, 123^{PE}, 124, 126, 128, 134, 143	(11) CDE102^{SEM}, 104$^{PE, SEM}$, 109, 110, 116, 117, 118^{SEM}, 119^{PE}, 129, 131$^{PE, SEM}$, 135	**44**
Santa Creu de Rodes (SCR)	(0)	(0)	(0)	(0)	(0)	(3) SCR001, 005^{PE}, 006^{PE}	(3) SCR002$^{PE, SEM}$, 003, 004	**6**
Torre Lardera (TLB)	(0)	(0)	(0)	(0)	(2) TLB001, 002	(0)	(0)	**2**
Camp del Rei (CDR)	(0)	(0)	(0)	(0)	(0)	(2) CDR001^{PE}, 002$^{PE, SEM}$	(0)	**2**
Vilarnau (VIL)	(0)	(0)	(0)	(1) VIL001	(0)	(0)	(2) VIL002, 003^{PE}	**3**
Total	**1**	**5**	**9**	**3**	8	**18**	**16**	**60**

Individuals from the ARQUB database PGR005, 006 and 007 have also been analysed by petrography, and PGR006 also by SEM.

Table 2
Mean ($\bar{X}$) and standard deviation (s) of the defined groups and concentrations of CDE149 and 151 loners (on normalised data). *tv*: total variation. Major and minor elements are expressed in *w*%. Trace elements are expressed in *w* mg/kg.

	CGEM01 ($n = 16$) ($tv = 0.14$)		**CGEM02** ($n = 12$) ($tv = 0.16$)		**CGEM03** ($n = 4$) ($tv = 0.14$)		**CGEM04** ($n = 2$) ($tv = 0.14$)		**CGROS01** ($n = 9$) ($tv = 0.33$)		**CGPGR01** ($n = 5$) ($tv = 0.25$)		**CDE149**	**CDE151**
	$\bar{X}$	s	$\bar{X}$	s	$\bar{X}$	s	$\bar{X}$	s	$\bar{X}$	s	$\bar{X}$	s		
Na_2O	0.81	0.09	0.87	0.13	1.21	0.13	1.45	0.12	1.52	0.20	2.59	0.15	2.54	2.75
MgO	1.63	0.10	1.36	0.19	1.28	0.13	1.65	0.01	1.42	0.22	1.17	0.06	1.30	1.69
Al_2O_3	20.36	0.62	20.32	0.80	18.73	0.78	16.53	0.55	17.45	1.23	17.44	0.58	17.48	19.85
SiO_2	63.90	0.91	63.51	1.57	65.93	1.70	67.44	0.46	68.25	2.06	67.98	0.80	67.47	61.97
K_2O	3.01	0.24	3.42	0.24	3.38	0.14	3.28	0.01	3.43	0.31	2.99	0.18	3.32	3.05
CaO	0.60	0.12	0.80	0.09	0.90	0.14	1.83	0.40	1.18	0.27	1.66	0.11	2.58	4.21
TiO_2	0.94	0.03	0.85	0.04	0.72	0.05	0.69	0.02	0.65	0.07	0.63	0.03	0.54	0.66
V	174	9	176	12	159	18	156	16	91	13	76	7	50	60
Cr	120	9	114	9	106	8	122	21	73	11	40	5	113	20
MnO	0.09	0.01	0.08	0.01	0.05	0.01	0.07	0.00	0.05	0.01	0.04	0.01	0.05	0.06
Fe_2O_3	8.41	0.25	8.53	0.47	7.56	0.65	6.81	0.44	5.87	0.67	5.36	0.24	4.52	5.58
Ni	61	4	58	8	52	5	62	12	32	7	18	3	52	6
Zn	105	10	92	11	86	7	90	6	73	10	59	3	45	63
Ga	23	1	23	2	21	1	18	1	20	2	19	1	20	24
Rb	118	7	122	16	112	3	113	2	132	19	106	7	123	135
Sr	83	14	86	9	100	11	120	1	100	19	144	2	156	205
Y	37	2	34	2	30	1	31	0	33	5	28	3	26	35
Zr	215	12	193	10	169	8	164	5	197	33	200	21	317	253
Nb	20	1	20	1	17	1	16	1	18	2	17	1	19	20
Ba	1655	161	1473	138	1423	62	1416	30	838	180	712	17	785	855
Ce	96	6	93	6	75	7	74	6	81	9	80	18	94	124
Pb	28	2	28	1	26	2	24	1	25	2	24	1	20	19
Th	17	1	18	1	15	1	14	1	17	2	19	0	17	20

performed using the same parameters and subcomposition as in the previous case, places individuals CDE149 and 151 (labelled with green arrows) out of the CGPGR01 group. Nevertheless, this is due to the differences in those individuals in their relative concentrations of CaO, Ni and Cr compared to the 5 Visigoth ceramics, as shown in the boxplot in Fig. 3, upper right corner. The remaining 15 ungrouped individuals will be considered loners.

The 5 defined groups are divided into two different branches of the dendrogram. On the left-hand side—highlighted in various shades of blue (Fig. 3)—four groups have been identified with the labels CGEM01, 02, 03 and 04, as all of them are composed of individuals recovered in archaeological sites belonging to the southern County of Empúries: EMP, CDE, and SCR. Except for the reference group CGEM04, composed of the only two cooking plaques recovered in CDE, no relationship between the chemical groups and the ceramic types could be observed. CDE109 and 137 have not been considered one chemical group, even if their association in the dendrogram is considerably low. The extreme similarity of their chemical composition and formal aspect, and the fact that they were recovered in the same archaeological context (Table 1 of the Supplementary Material), makes us consider that they could belong to the same vessel even if they are non-adjoining sherds. On the right-hand branch, only one chemical group (labelled as CGROS01 and highlighted in pink) has been defined. This group contains all the individuals recovered in the northern County of Rosselló (CDR and VIL) and some individuals corresponding to southern archaeological sites (EMP503, CDE129, 135, and 154). As can be seen in the dendrogram, CGROS01 is less homogeneous than CGEM chemical groups.

For a better understanding of the chemical differences in the studied set, we performed the singular value decomposition of the double-centred clr transformed data (Aitchison and Greenacre, 2002;

Table 3
Summary of the mineralogical fabrics defined by XRD for each chemical group. These fabrics are contrasted with the vitrification stage assessed by SEM. The EFT is estimated from XRD and SEM observation. The petrographic fabrics are also displayed. n: number of individuals; Afs: alkali feldspar; Cal: calcite; Hem: hematite; Ilt: illite-muscovite; Kln: kaolinite; Mor: mordenite; Pl: plagioclase; Qz: quartz; Spl: spinel; Tlc: talc (abbreviations according to Whitney and Evans, 2010). NV: no vitrification; IV: initial vitrification; V: extensive vitrification; TV: total vitrification; FH: fast-heating; EFT: equivalent firing temperature. [SEM]: individual examined by SEM. [PE]: individual examined by petrography.

PXRD Fabric	Mineralogic assemblage	Individuals	Vitrification stage	EFT (°C)	Petrographic fabric	Figures
CGEM01 ($n = 16$)						
CGEM01-F1 ($n = 2$)	Ilt, Pl, Afs, Qz, Tlc	CDE123[PE], 150[SEM]	NV	< 750	PEM02	5, a
CGEM01-F2 ($n = 2$)	Ilt, Pl, Afs, Qz, Tlc, Hem	CDE139, 148[SEM]	NV	< 750		
CGEM01-F3 ($n = 2$)	Ilt, Pl, Afs, Qz, Hem	CDE131[SEM, PE], SCR006[PE]	NV	< 750	PEM02	6, a
CGEM01-F4 ($n = 3$)	Ilt, Pl, Afs, Qz, Spl	CDE117, SCR001, 005[SEM, PE]	V	≈ 900	PEM02	6, b; 7, d
CGEM01-F5 ($n = 6$)	Ilt, Pl, Afs, Qz, Hem, Spl	CDE118[SEM], 134, 143, 152, 153, SCR002[SEM, PE]	V	≈ 900	PEM02	5, b; 6, c
CGEM01-F6 ($n = 1$)	Ilt, Pl, Afs, Qz, Hem, Spl, Mor?	CDE155[SEM]	V	≈ 900		5, c
CGEM02 ($n = 12$)						
CGEM02-F1 ($n = 2$)	Ilt, Pl, Afs, Qz, Hem, Tlc, Kln?	CDE102[SEM], 113	NV	< 750		5, d
CGEM02-F2 ($n = 7$)	Ilt, Pl, Afs, Qz, Hem, Tlc	CDE108, 120, 124, 141, 145, 146, EMP501[SEM, PE]	NV	< 750	PEM02	6, d
CGEM02-F3 ($n = 2$)	Ilt, Pl, Afs, Qz, Hem	CDE116, 142[SEM]	V	800–900		
CGEM02-F4 ($n = 1$)	Ilt, Pl, Afs, Qz, Hem, Spl	CDE115[SEM, PE]	V	≈ 900	PEM02	6, e; 7, f
CGEM03 ($n = 4$)						
CGEM03-F1 ($n = 2$)	Ilt, Pl, Afs, Qz, Tlc, Hem	CDE104[SEM, PE], 136	NV	< 750	PEM02	6, f
CGEM03-F2 ($n = 2$)	Ilt, Pl, Afs, Qz, Tlc	CDE119[PE], 144[SEM]	NV	< 750	PEM02	7, e
CGEM04 ($n = 2$)						
CGEM04-F1 ($n = 2$)	Ilt, Pl, Afs, Qz, Cal, Tlc?, Hem?	CDE101[SEM, PE], 112[PE]	NV	< 750	PEM01	7, c
CGROS01 ($n = 9$)						
CGROS01-F1 ($n = 2$)	Ilt, Pl, Afs, Qz, Tlc, Cal?	CDE135, CDR001[SEM, PE]	NV	< 750	PROS01	7, a
CGROS01-F2 ($n = 1$)	Ilt, Pl, Afs, Qz, Tlc, Hem, Cal?	CDR002[SEM, PE]	NV-IV	< 750–800	PROS01	
CGROS01-F3 ($n = 5$)	Ilt, Pl, Afs, Qz, Cal?	CDE129, 154, VIL001, 002[SEM], 003[PE]	IV	750–800	PROS01	6, g
CGROS01-F4 ($n = 1$)	Pl, Afs, Qz, Spl	EMP503[SEM, PE]	TV (FH)	> 950/ 1000	PPGR01	5, e; 6, h
Loners-PGR						
CDE149	Ilt, Pl, Afs, Qz, Cal?	CDE149[SEM, PE]	NV	< 750	PEM01	
CDE151	Ilt, Pl, Afs, Qz, Cal	CDE151[SEM, PE]	V	≈ 800	PEM03	5, f; 6, i
CGPGR01 ($n = 5$)						
CGPGR01-F1 ($n = 5$)	Ilt, Pl, Afs, Qz	PGR003, 004, 005[PE], 006[SEM, PE], 007[PE]	NV	< 750	PPGR01	7, b

Greenacre, 2010; van de Boogaart and Tolosana-Delgado, 2013) on the 60 individuals studied, plus those 5 recovered at PGR. The two first principal components in the covariance and form biplots (Fig. 4) explain more than 75 % of the variance (VE = 77.13 %). The first principal component explains most of the variance (VE = 69.00 %) and shows the relative values of CaO, Na_2O and Sr on the left-hand side and Ni, Cr, V, Ba and MnO on the right-hand side. These components are the most involved in group formation, as can be understood from the compositional evenness graph (Fig. 2). Along this first principal component, the biplots show a clear division between chemical groups CGEM01, CGEM02, CGEM03, and CGEM04 (on the right-hand side) and chemical groups CGROS01 and CGPGR01 (on the left-hand side). The main differences between both areas are explained by the general increase of CaO, Na_2O and Sr relative content towards the left-hand side (Table 2). Contrariwise, Ni, Cr, V, Ba and MnO relative values are lower in CGROS01 and CGPGR01, generally increasing towards the right-hand side. In particular, the values of Ba for groups CGEM01, CGEM02, CGEM03, and CGEM04 must be considered significantly high (Table 2). The second principal component (VE = 8.13 %) is mainly determined by the influence of CaO, Ni and Cr relative values, which are placed on the upper part. The location of group CGEM04 on the upper part of this second principal component is possibly due to the high relative value in CaO within the CGEM groups. Finally, it is important to notice the significantly high concentrations of Na_2O in CGPGR01, which place this group in the extreme left area of the biplot.

Individuals CDE149 and 151 (labelled for convenience "loners-PGR" in the text hereafter) also exhibit significantly high relative values of Na_2O (Fig. 4). They are placed at the left end because of their extremely high Na_2O concentrations (2.54 % and 2.75 %, respectively) (Table 2), similar to those observed in PGR individuals (with a mean value of 2.59 % ± 0.15 %). Despite this similarity, individuals CDE149, at the upper part, and CDE151, at the lower part, are separated in the second principal component because of their differences in CaO (2.58 % and 4.21 %, respectively), Ni (52 mg/kg and 6 mg/kg) and Cr relative concentrations (113 mg/kg and 20 mg/kg); as it could also be noticed in Fig. 3, upper right corner.

3.2. Mineralogical and microstructural analysis

Chemical results show that the individuals analysed correspond to ceramics technically considered low calcareous, *i.e.*, CaO < (5–6)%. For these ceramics, XRD and SEM results may enable the estimate of the equivalent firing temperatures (EFT) after the mineralogical scales and changes in the microstructure and the firing conditions (Roberts, 1963; Picon, 1973; Tite et al., 1982; Heimann and Maggetti, 2014; Buxeda i Garrigós and Madrid i Fernández, 2016a; Gliozzo, 2020).

The study of the XRD diffractograms (Fig. 5, Table 3) enables the identification of six different fabrics in group CGEM01. Fabrics CGEM01-F1, CGEM01-F2 and CGEM01-F3 are characterised by the absence of spinel, a typical firing phase which crystallises around 900 °C in low calcareous ceramics with a MgO content between (1–2)% and (6–7)%. These fabrics also exhibit illite-muscovite, quartz, plagioclase and alkali feldspar, but only fabrics CGEM01-F1 and CGEM01-F2 exhibit talc (Fig. 5, a), which is thermally decomposed at 800 °C when being

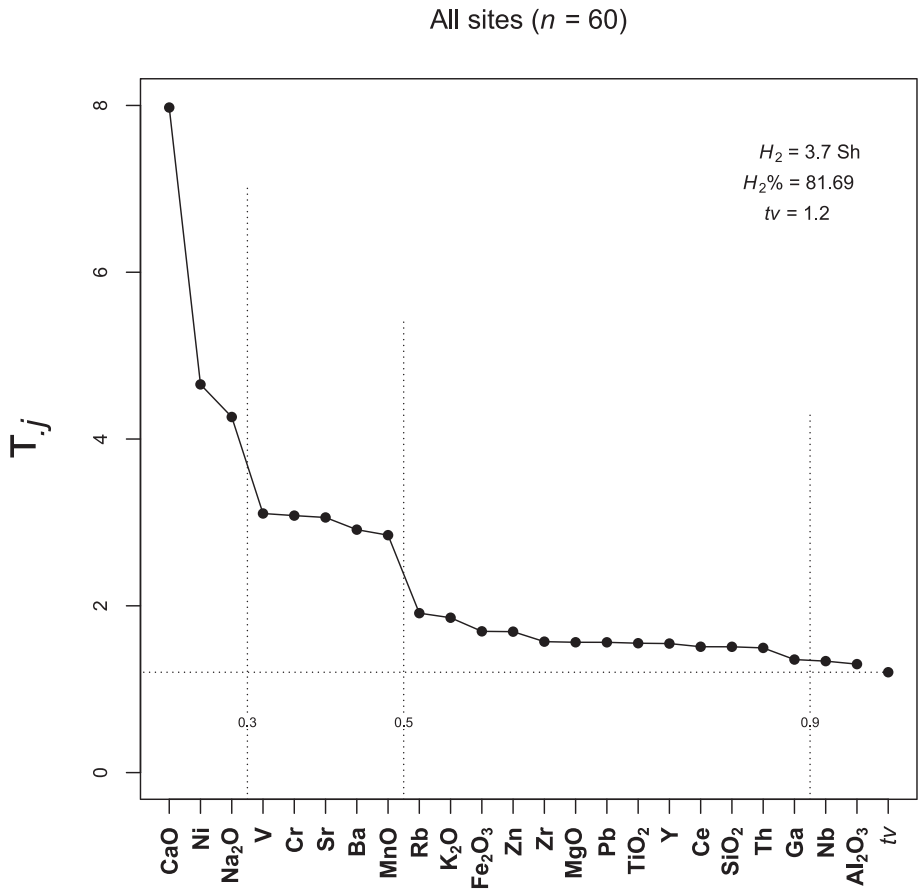

Fig. 2. Compositional evenness graph of the 60 studied individuals. H_2: information entropy (in shannons, Sh); H_2%: percentage of the maximum possible attainable; *tv*: total variation; $\tau_{.j}$: trace of the variance–covariance matrix following the alr transformation using element *j* as the divisor. Vertical dotted lines express different *tv*/$\tau_{.j}$ values.

transformed into enstatite (Liu et al., 2014; Maritan et al., 2018), while fabrics CGEM01-F2 and CGEM01-F3 exhibit hematite. Their study by SEM shows a no vitrification microstructure (NV) (Fig. 6, a), indicating an EFT below 750 °C. Fabrics CGEM01-F4, CGEM01-F5 and CGEM01-F6 show the crystallisation of spinel together with the presence of illite-muscovite pointing to an EFT between 900 °C and 950/1000 °C (Fig. 5, b). Most probably, the crystallisation of spinel prevents the observation of enstatite after talc transformation. The difference between fabrics CGEM01-F4 and CGEM01-F5 is hematite, present only in the latter. Fabric CGEM01-F6 exhibits a pretty intense peak at 3.44 Å (25.84°2θ) that seems to correspond to the $d_{(1\,2\,2)}$ peak (I% = 100) of mordenite (JCPDS #00–022-1340; $(Na_2,Ca,K_2)_4(Al_8Si_{40})O_{96}{\cdot}28H_2O$) (mordenite has also been reported by Borgers et al., 2021) (Fig. 5, c). This zeolite must be a secondary phase since this mineral decomposes at 600 °C (Pechar and Rykl, 1987). The study by SEM of these high-temperature fabrics shows an extensive vitrification stage (V) characteristic for low calcareous pastes of an EFT in the range 800–900 °C (Fig. 6, b and c) (Heimann and Maggetti, 2014, 97).

The evolution of the firing phases for GCEM02 shows a similar development to the previous group, although only four different fabrics have been identified in this case. The first two, GCEM02-F1 and GCEM02-F2, show the presence of talc, pointing to an EFT below 800 °C, and only the GCEM02-F1 presents one peak that could correspond to kaolinite (Fig. 5, d). The study by SEM of these two fabrics exhibits a stage of no vitrification (NV), enabling us to estimate an EFT below 750 °C (Fig. 6, d). The lack of talc and spinel characterises fabric GCEM02-F3, suggesting an EFT in the range of 800–900 °C, in close agreement with the extensive vitrification stage (V) observed by SEM. Finally, fabric GCEM02-F4 shows, besides the absence of talc, the presence of spinel and illite-muscovite, pointing to an EFT at 900–950 °C, in concurrence with the higher range of the extensive vitrification stage (V) observed by SEM (Fig. 6, e) suggesting an EFT around 900 °C.

The diffractograms of group CGEM03 are divided into two fabrics according to the presence or absence of hematite. The presence of talc characterises both fabrics, and the EFT can be estimated below 800 °C. The observations by SEM also show a no vitrification stage (NV) of the matrix, lowering the estimated EFT below 750 °C (Fig. 6, f).

Regarding group CGEM04, only one fabric can be identified. Besides illite-muscovite, plagioclase, alkali feldspar, and quartz, the presence of talc and hematite seems possible, although their peaks are not intense enough for clear identification. However, the most singular characteristic is the presence of calcite, which could explain the higher CaO content of this group (Table 3). The observation by SEM shows a no vitrification stage (NV), enabling the estimate of the EFT below 750 °C.

For the last group defined, CGROS01, four fabrics were identified. Illite-muscovite, plagioclase, alkali feldspars, and quartz are present in all individuals. Moreover, calcite is also possibly present, but the low intensity of the main peak makes identification difficult in several cases. Fabrics CGROS01-F1 and CGROS01-F2 are characterised by talc and differ by the presence of hematite in individual CDR002. The presence of talc enables estimating the EFT below 800 °C, in agreement with the SEM's observation, which shows a no vitrification (NV) or initial vitrification (IV) stage, pointing again to an EFT below 750 °C or 800 °C. Fabric CGROS01-F3 does not show talc or spinel. Moreover, the presence of calcite might suggest an EFT below 800–850 °C, and the initial vitrification (IV) stage enables estimating the EFT between 750 °C and 800 °C (Fig. 6, g). Finally, the individual EMP0503 (fabric CGROS01-F4) exhibits distinctive characteristics, such as spinel's presence and illite-

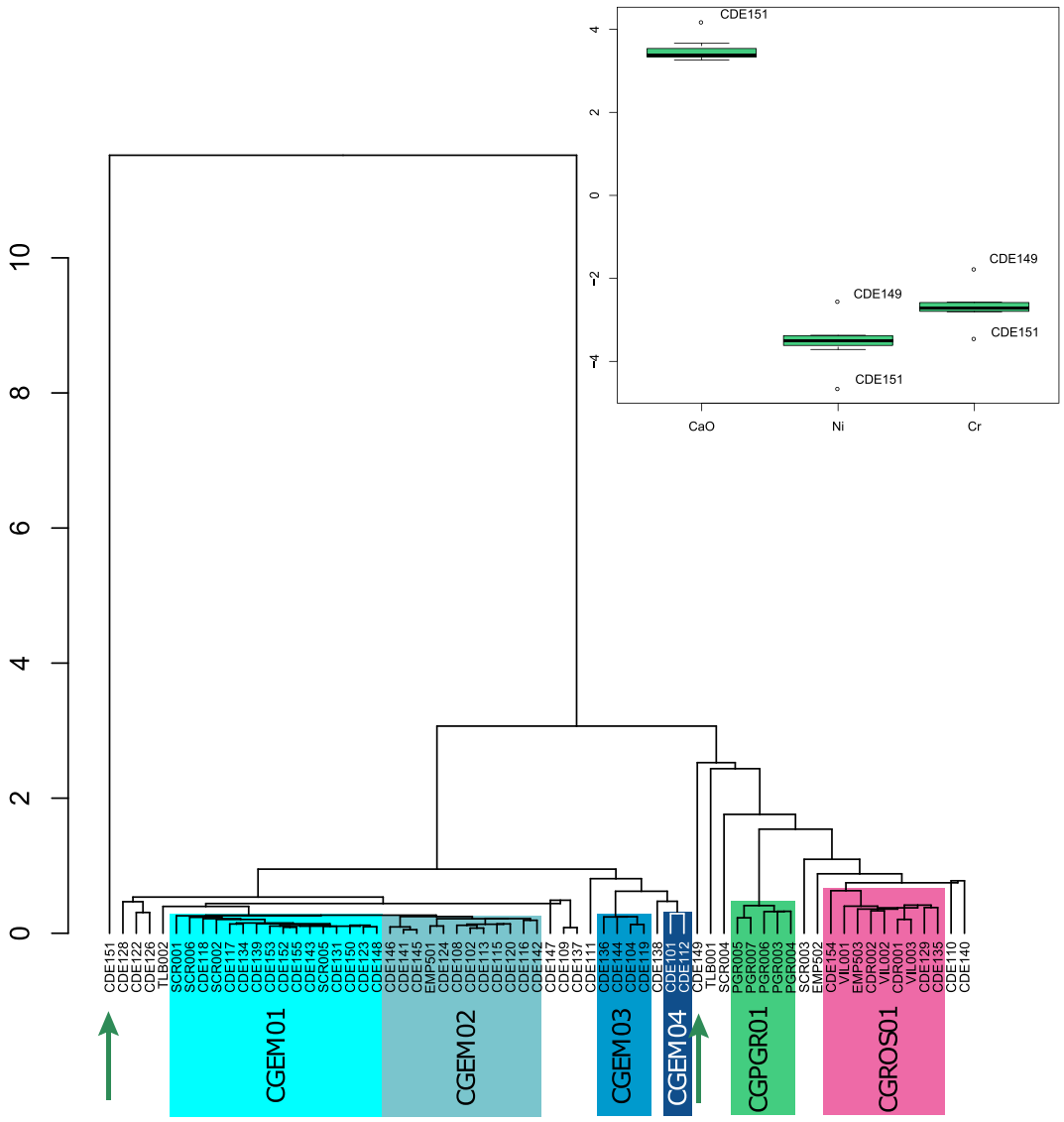

Fig. 3. Dendrogram from the cluster analysis on the Na_2O, MgO, Al_2O_3, SiO_2, K_2O, CaO, TiO_2, V, Cr, MnO, Fe_2O_3, Ni, Zn, Sr, Ce, Zr, Nb, and Ba subcomposition clr transformed of the 60 individuals analysed in this study, compared with 5 relevant individuals of the ARQUB database corresponding to the archaeological site of Puig-Rom (PGR). Green arrows: Individuals recovered at Castelló d'Empúries archaeological site and related to CGPGR01 reference group. Upper right corner: boxplot of the CaO, Ni and Cr clr transformed values for the CGPGR01 reference group together with individuals CDE149 and 151. (For interpretation of the references to colour in this figure legend, the reader is referred to the web version of this article.)

muscovite's absence, suggesting an EFT over 950/1000 °C (Fig. 5, e). SEM observation confirms this by exhibiting a microstructure characteristic of a total vitrification stage (TV) (Fig. 6, h) (Heimann and Maggetti, 2014, 98). This total vitrification stage in low calcareous pottery allows estimating an EFT over 900 °C. It is also interesting to remark on the presence of many micro-bloating pores below 5 μm in size, characteristic of a fast-heating process, usually corresponding to bonfire firing (Buxeda et al., 2003).

Observing the diffractograms for CGPGR01 and loners-PGR (CDE149 and CDE151), it is clear that they exhibit more intense peaks of plagioclase (Fig. 5, f) in clear correspondence with the extremely high Na_2O content. The fabrics of loners-PGR and CGPGR01-F1, the only fabric of this chemical group, exhibit the same mineral phases, except for calcite, solely observed in loners-PGR, as expected after their higher CaO content (Table 3). Talc is never observed, and the absence of clear firing phases suggests low EFT (Table 3). The observations by SEM show no vitrification (NV) stage for individuals CDE149 and PGR006, enabling to estimate an EFT below 750 °C, while extensive vitrification (V) is observed for individual CDE151 (Fig. 6, i). This vitrification stage, together with the presence of calcite, points to an EFT close to 800 °C for this latter individual. Thus, the low EFT estimated for these ceramics suggests that talc might not be present in their raw materials, contrary to the previous groups.

Finally, the remaining 15 loners can be discussed following the two main branches of the dendrogram in Fig. 3. Nine individuals are placed on the left branch. From those, individuals TLB002 and CDE111 exhibit diffractograms similar to those of the low EFT of the previous groups (except loners-PGR and CGPGR01), including talc. Individual TLB002 also exhibits hematite and calcite. The EFT estimated for both individuals is below 800 °C. Individuals CDE109, 122, 126, 128, 137 and 147 do not show talc and contain spinel and illite-muscovite, pointing to an EFT between 900 °C and 950 °C. Individuals CDE122, 126 and 147 also exhibit hematite. Finally, individual CDE138 do not show talc nor spinel. Even if the EFT could be estimated between 800 °C and 900 °C, the only secure estimation is below 950/1000 °C after the presence of illite-muscovite. It should be highlighted that individuals CDE109 and 138 also exhibit the possible peak already discussed for mordenite. Regarding the 6 loners on the right branch of the dendrogram (CDE110,

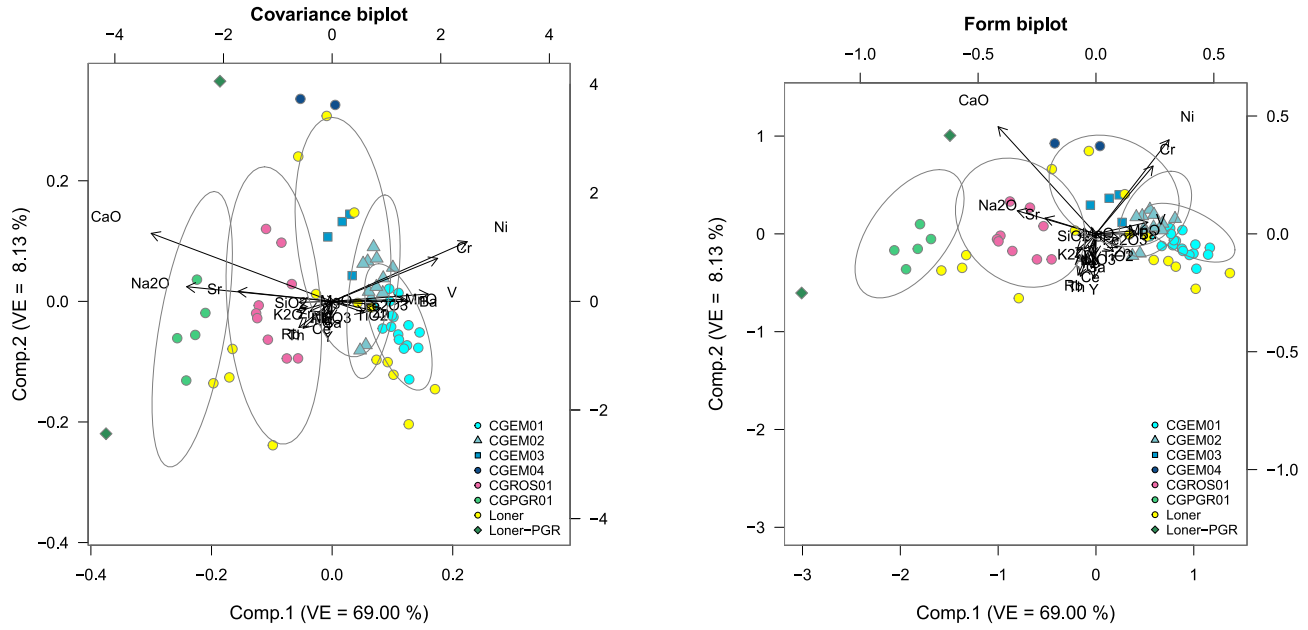

Fig. 4. Covariance (left) and form (right) biplots of the singular value decomposition on the subcomposition Na_2O, MgO, Al_2O_3, SiO_2, K_2O, CaO, TiO_2, V, Cr, MnO, Fe_2O_3, Ni, Zn, Sr, Ce, Zr, Nb, and Ba, double centred clr transformed. VE: variance explained. For groups of more than 3 individuals, the 0.95 probabilistic ellipsoids are shown.

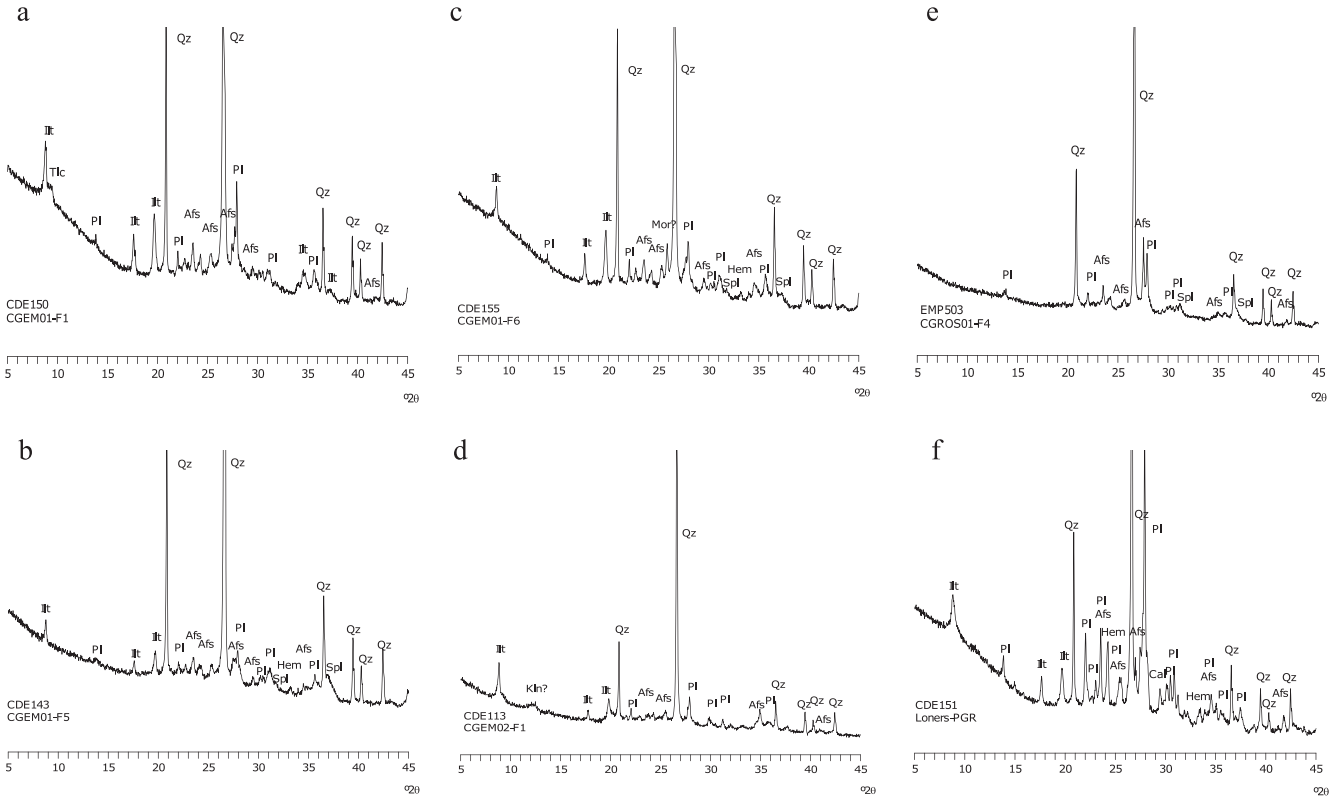

Fig. 5. XRD patterns for the categories of association of crystalline phases as detected by XRD. a) individual CDE150, fabric CGEM01-F1; b) individual CDE143, fabric CGEM01-F5; c) individual CDE155, fabric CGEM01-F6; d) individual CDE113, fabric CGEM02-F1; e) individual EMP503, fabric CGROS01-F4; f) individual CDE151, loner-PGR. Afs: alkali feldspar; Cal: calcite; Hem: hematite; Ilt: illite-muscovite; Kln: kaolinite; Mor: mordenite; Pl: plagioclase; Qz: quartz; Spl: spinel; Tlc: talc (abbreviations according to Whitney and Evans, 2010).

140, TLB001, EMP502, SCR003 and 004), all of them are similar to the ones with low EFT exhibiting talc: individuals CDE140 and TLB001 exhibit calcite and EMP502 hematite. Again, the EFT must be estimated below 800 °C.

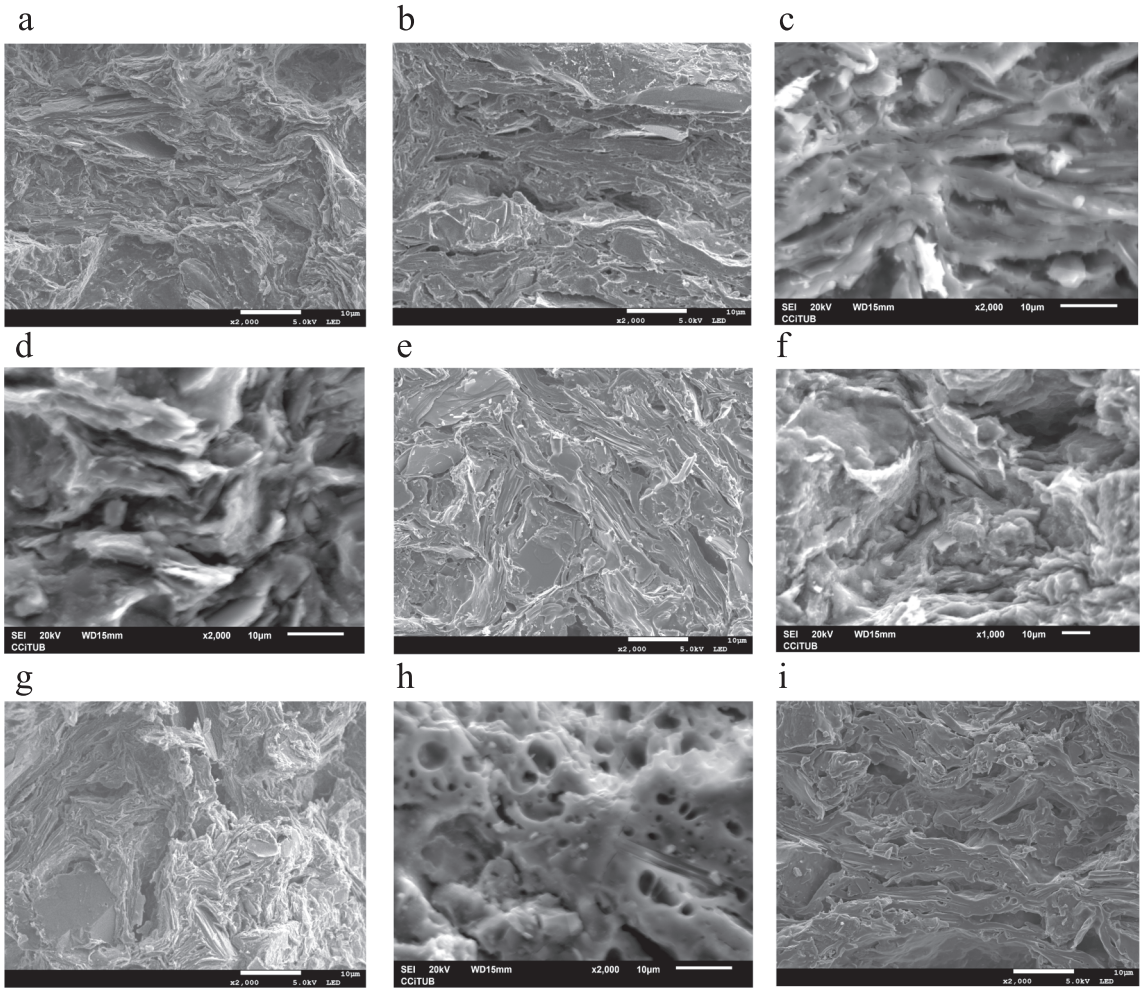

Fig. 6. Photomicrographs by SEM. a) individual CDE131, fabric CGEM01-F3, NV stage; b) individual SCR005, fabric CGEM01-F4, V stage; c) individual SCR002, fabric CGEM01-F5, V stage; d) individual EMP501, fabric GCEM02-F2, NV stage; e) individual CDE115, fabric GCEM02-F4, V stage; f) individual CDE104, fabric CGEM03-F1, NV stage; g) individual VIL002, fabric CGROS01-F3, IV stage; h) individual EMP503, fabric CGROS01-F4, TV stage and FH; i) individual CDE151, loner-PGR, V stage. NV: no vitrification; IV: initial vitrification; V: extensive vitrification; TV: total vitrification; FH: fast-heating.

3.3. Petrographic examination

The 21 individuals selected for the petrographic analyses have been grouped into 4 fabrics (Table 3 and Table 2 of the Supplementary Material, Fig. 7).

Fabric PROS01 (Fig. 7, a) includes some of the individuals in the chemical group CGROS01, and it is characterised by moderately sorted inclusions of mainly monocrystalline quartz and alkali feldspars; the larger fraction includes polycrystalline quartz, sand/siltstones and granite rock fragments. The size distribution is skewed unimodal, with most of the coarse fraction in the range of the medium-very fine sands with a few larger inclusions heterogeneously distributed along the section. The coarse fraction is related to a mixed sedimentary-acid igneous environment, as it could be found in the western part of the Pyrenees (IGME, 2008). Even though the number of individuals is too low to determine provenance, the PROS01 fabric lacks a medium–high grade metamorphic component present in the other fabrics and, therefore, could be provisionally considered characteristic of the area of the County of Rosselló.

The individuals from the chemical group CGPGR01 and individual EMP503 (chemical group CGROS01) show features that allow them to group in one fabric, PPGR01 (Fig. 7, b). This fabric is composed of poorly sorted inclusions, mainly large fragments of high-grade metamorphic rocks (mylonite and gneiss) and large alkali feldspars phenocrystals and monocrystalline quartz, these last two probably deriving from gneiss or granite (pegmatite) rocks of which some fragments are present; large fragments of plagioclase feldspars identified as albite are also present. Some low-grade metamorphic rocks are present in the individuals PGR006 and EMP503. This last individual is temporarily included in this group for the similarity in the coarse fraction, while from the chemical results, it was included in the CGROS01 group. Inclusion size distribution is bimodal, with the coarse fraction ranging from very coarse to medium sand, and it is generally homogeneously distributed along the section. The coarse fraction seems to be added to a finer paste. Fine fraction is in the range of fine sand to coarse silt size range and is homogeneously distributed. This fabric shares with PROS01 the presence of granite inclusions, but the other aplastic fraction of PPGR01 is related to a high-grade metamorphic environment mixed with acidic igneous rocks, which are common in the south of Pyrenees (IGC, 2006). Specifically, the presence of mylonite and pegmatite fragments points out for the area of Cap de Creus (Fort i Costa 2006; Carreras Planells et al., 1994a) as the possible area of formation of the raw materials present in this fabric. Furthermore, a similar composition has been found in some mortars from the medieval walls of PGR (Fernández Lara, 2021).

Fabric PEM01 includes all the individuals grouped into the chemical group CGEM04 and the loner-PGR CDE149. The fabric PEM01 (Fig. 7, c) is composed of poorly sorted inclusions, mainly alkali feldspars phenocrystals and large monocrystalline quartz together with fragments of gneiss and granite as the PPGR01 fabric; in contrast from that, this fabric also includes metamorphosed limestone and some well-rounded

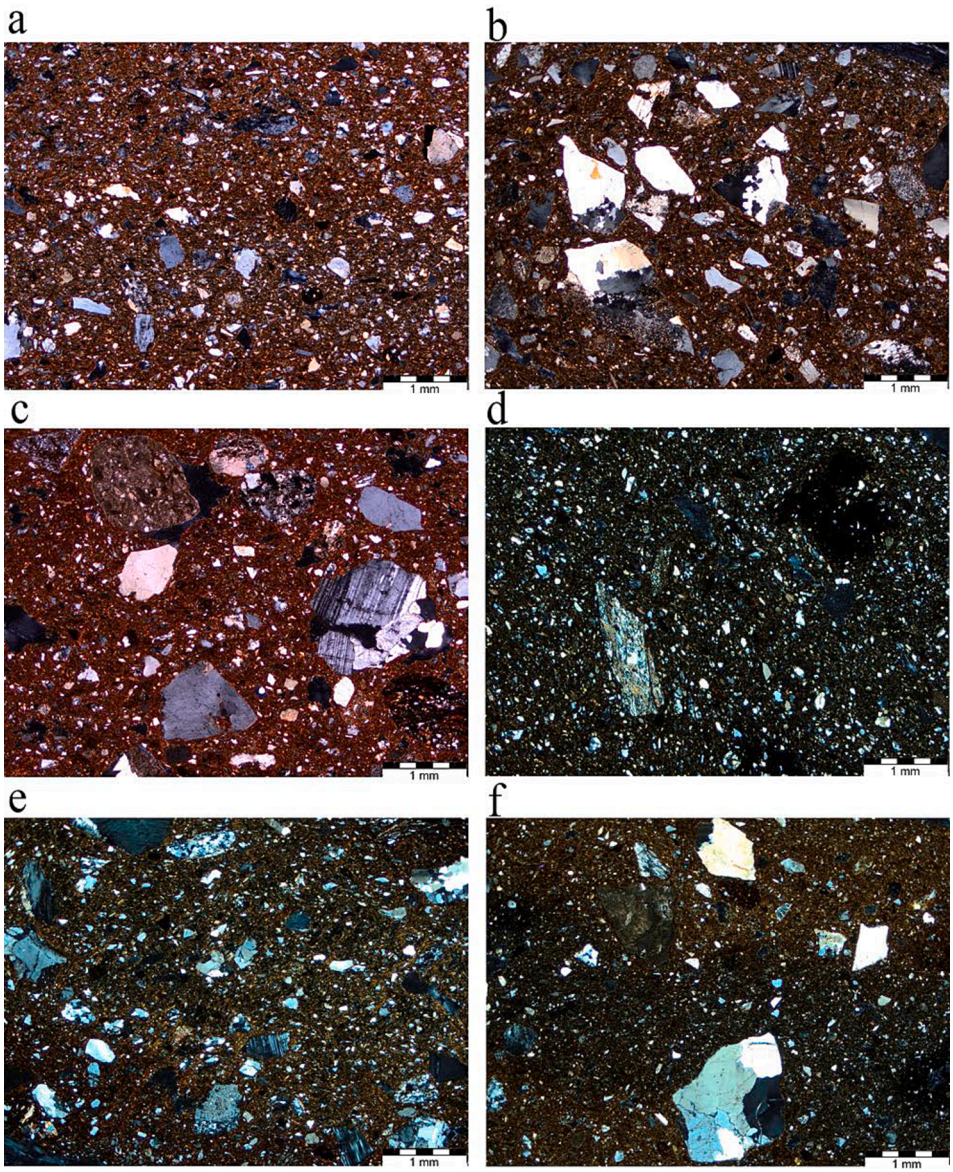

Fig. 7. Photomicrographs (XP) of the most representative individuals for each petrographic fabric: a) CDR001, fabric PROS01; b) PGR006, fabric PPGR01; c) CDE101, fabric PEM01; d) SCR005, fabric PEM02; e) CDE119, fabric PEM02; f) CDE115, fabric PEM03.

sedimentary rock fragments (micritic limestone and siltstones). Some large fragments of muscovite and biotite mica are also present. Inclusion size distribution is bimodal, with the coarse fraction ranging from very coarse to medium sand, and it is generally homogeneously distributed along the section. Fine fraction is in the range of fine sand to coarse silt size range and is homogeneously distributed. The presence of this mixture of rock fragments, some of them well-rounded, suggests the provenance for these individuals not far from the previous group but probably in correspondence with some riverbed which might have transported and mixed some of the rock formations of the southern Pyrenees. CDE, where these individuals were found, stands above the river Muga and provisionally, we might suggest this as a possible provenance area for these individuals.

Compared to the previous one, fabric PEM02 has a finer texture of moderately sorted inclusions of monocrystalline quartz, metaquartzite and low-medium grade metamorphic rocks (chlorite phyllite to schist with visible crenulation and schistosity developed). The finer fraction includes the same chlorite mica observed in the metamorphic rock fragments. Inclusion size distribution is unimodal to skewed unimodal as some individuals show a larger fraction: overall, the fraction size ranges from fine to medium sand size, homogeneously distributed along the section, with a few larger clasts of very coarse sand to pebble size heterogeneously distributed along the section. Generally, the SCR individuals have a finer texture than the CDE individuals, but they have been grouped, as they show the same rock fragment ranges (Fig. 7, d-e). This fabric includes all the individuals of the chemical groups CGEM01, CGEM02, CGEM03 and the loner CDE122. The presence of chlorite phyllite to schist is related to the chlorite-muscovite metamorphic zones present to the north of Cap de Creus, up to Portbou, and the south-western part of the cape (Carreras Planells et al., 1994a, b). Considering the location of the settlements where the individuals were found, CDE, EMP and SCR, we might provisionally consider the southern-western foothill of Cap de Creus as a possible area of provenance of the raw mateterials for the individuals in this fabric.

The last fabric, PEM03 (Fig. 7, f), includes only one individual, the loner-PGR CDE151, which shows some similarities to the CGPGR01 chemical group, though it is unclear to group it within it. This fabric comprises moderately sorted alkali feldspars and quartz inclusions, with larger inclusions of micritic mudstones, metaquartzite and granite rock fragments. Most of the inclusions range in the fine to very fine sand size

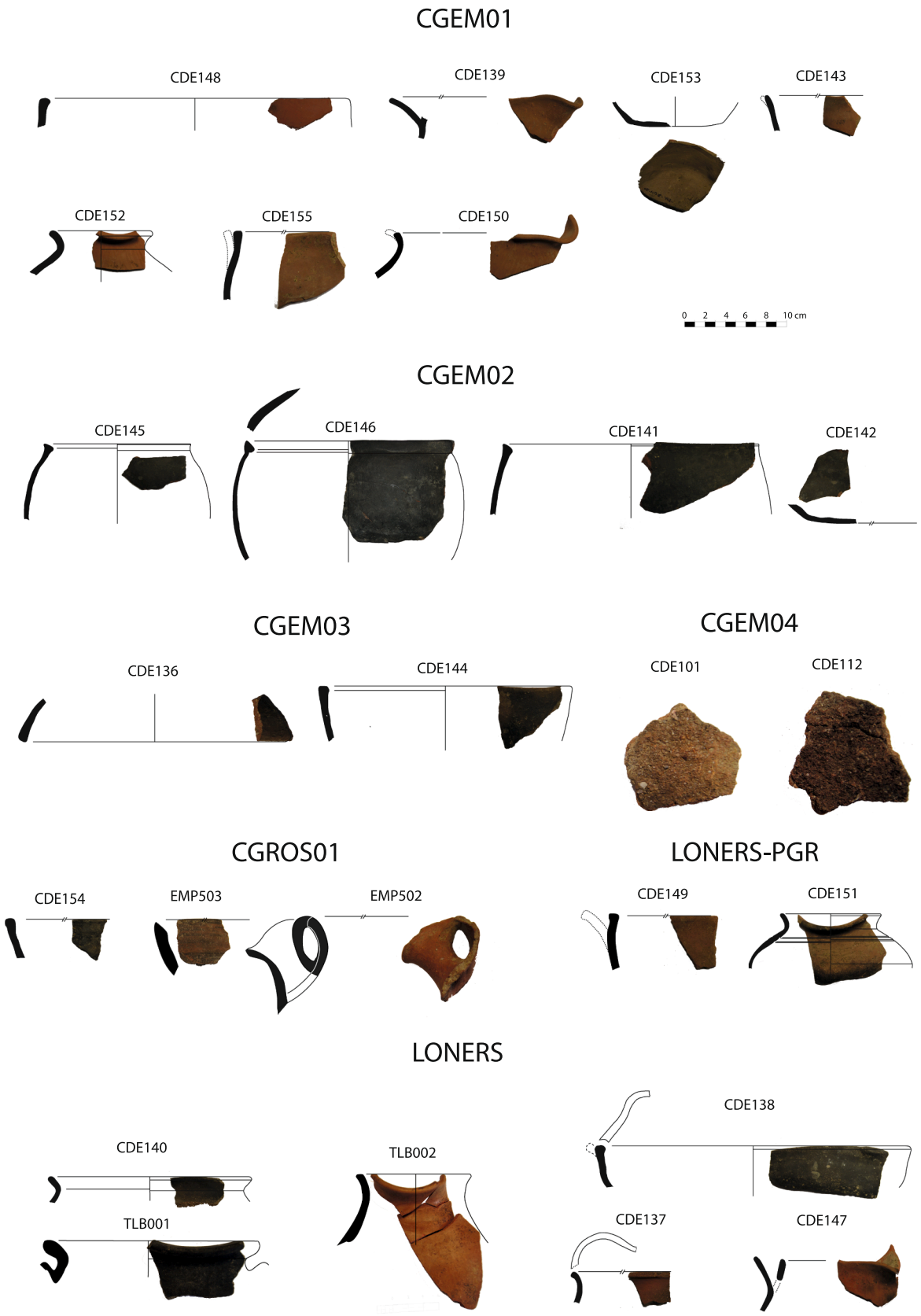

Fig. 8. Drawings and pictures of representative ceramics for each one of the defined groups and some loners.

and are homogeneously distributed along the section, while a few larger inclusions ranging from very coarse to medium sand are heterogeneously distributed along the section. The grain size distribution is considered skewed unimodal. A few vesicle voids, with black rims, a sign of burnt organics, and rare *meso*-vughs are present. Inclusions and voids show random orientation. Compared to the previous ones, this fabric is less micaceous than PEM01 and PEM02 and with more calcareous components than PPGR01; amongst the inclusions, it strikes the presence of micritic mudstone and the absence of low-grade metamorphic rocks. Despite these differences, the provenance can be considered generically from the same area.

4. Discussion

The results obtained allowed us to define 5 chemical groups and up to 17 loners, from which 2 show similarities with the Visigoth ceramics of group CGPGR01. All low-fired ceramics (except loners-PGR) exhibit the presence of talc, which might be evidence of regional provenance since the eastern Pyrenees host a large number of talc-chlorite mineralisations that occur through several processes, among which the hydrosiliphication of the Cambro-Ordovician marbles (very rich in magnesium). Talc mineralisation has been traditionally exploited at la Vajol (and the surrounding area), Vilajuïga (a village at the eastern end of Cap de Creus), and Ceret (Fig. 1) (Mata, 1990, 89; Boulvais et al., 2006; Boutin et al., 2016).

In contrast, loners-PGR and group CGPGR01 exhibit extremely high Na_2O concentrations (Table 3) that could be explained by the presence of the high sodium plagioclase albite ($NaAlSi_3O_8$) identified in pegmatite rocks belonging to the area of Cap de Creus. The identification of this mineral has also been confirmed in XRD analysis, where intense peaks of plagioclase can be observed in all the individuals classified in the CGPGR01 chemical group and loners-PGR. In the eastern Pyrenees, there is a geographically close match between talc/chlorites mineralisation and albitisation processes (Boulvais et al., 2007; Poujol et al., 2010). Those processes have implied the formation, in different environments and after different processes, of albitites in areas like Llançà or Argelers (Fig. 1), which can explain the Na_2O content of these ceramics. Most probably, the albitisation and talc mineralisation were two independent metasomatic events of a single, regional-scale, long-lived hydrothermal system (Poujol et al., 2010), and their relations with the results obtained in our study reinforce the local or regional origin of our defined groups and all, or most, of our loners.

On the one hand, the petrographic observations confirm that individuals belonging to CGROS01-PROS01 could be manufactured in the northern areas of the County of Rosselló. These lack that mixture of the metamorphic component and the igneous one in the aplastic fraction that characterises the other fabrics and can be considered produced on the southern part of the Pyrenees. On the other hand, those individuals belonging to CGPGR01-PPGR01 would have their origin nearby the area ofCap de Creus. Concerning CGEM chemical groups, petrography points out that the provenance of CGEM01, 02 and 03 chemical groups (united in PEM02 petrographic fabric) could be related to the south-western foothills of Cap de Creus and, in the case of CGEM04-PEM01, it would belong to a riverbed area, probably nearby the historical town of CDE. Finally, the only individual in PEM03 (CDE151) shares the rock fraction characteristics with others, allowing us to include it generically in the same area of provenance, but the paste seems more calcareous. The chemistry for loners-PGR CDE149 and 151 also suggests a necessary relation with the albitites and, possibly, with group CGPGR01.

Turning our attention to the ceramics from an archaeological point of view, it is clear that, despite chemical group CGEM04 (composed of the only two cooking plaques recovered in the southern area), no relevant relationship between the groups or fabrics and specific forms, surface treatments or chronologies could be observed (Table 4, left; Fig. 8). Focusing on the relation between the chemical groups defined and the sampled archaeological sites (Table 4, right) we can observe that all the individuals forming groups CGEM03 and CGEM04 and the loners-PGR have been recovered in CDE. The same could be stated for group CGEM02, except for 1 individual recovered at EMP. Chemical group CGEM01 is also related to CDE but comprises a large part of the individuals from SCR. The situation is very different for group CGROS01, including individuals recovered at four different sites: all individuals from the County of Rosselló (CDR and VIL) and CDE and EMP. Thus, no ceramics related to the southern part of the Albera range have been recovered so far in the County of Rosselló, but 4 out 9 individuals from group CGROS01, whose origin must be somewhere in this County, have been found in the southern part of this range, in the County of Empúries.

It must also be highlighted that, without considering the two loners-

Table 4
Chemical groups in relation to (left) ceramic class and (right) recovery site.

	Ceramic class								Recovery site					
	Sitra	Pitcher	Casserole and casserole cover	Cooking plaque	Cooking pot	Spatulated sherds	Coarse ware sherds	Total	EMP	CDE	SCR	TLB	CDR	VIL
CGEM01		CDE150, 152, 153, 155	CDE148		CDE139	CDE123, 134, 143, SCR001, 005, 006	CDE117, 118, 131, SCR002	**16**	0	12	4	0	0	0
CGEM02			CDE141, 142		CDE145, 146	EMP501, CDE108, 113, 115, 120, 124	CDE102, 116	**12**	1	11	0	0	0	0
CGEM03			CDE136, 144				CDE104, 119	**4**	0	4	0	0	0	0
CGEM04				CDE101, 112				**2**	0	2	0	0	0	0
CGROS01			EMP503, CDE154	VIL001		CDR001, 002	CDE129, 135, VIL002, 003	**9**	1	3	0	0	2	3
Loner-PGR			CDE149		CDE151			**2**	0	2	0	0	0	0
Loner	EMP502	CDE147	CDE138		CDE137, 140, TLB001, 002	CDE111, 122, 126, 128	CDE109, 110, SCR003, 004	**15**	1	10	2	2	0	0
Total	**1**	**5**	**9**	**3**	8	**18**	**16**	**60**	**3**	**44**	**6**	**2**	**2**	**3**

PGR, 15 individuals remain ungrouped. These individuals could belong to chemical groups only represented by themselves, which could grow if more individuals are analysed. With the information available until now, that would mean that a total of 22 paste reference compositional units (PCRUs) can be defined from a chemical point of view. Thus, the amount of possible PCRUs defined makes us think in a context determined by many production centres, mostly unknown, which implies the existence of a heterogeneous production and a local or, at most, a regional distribution.

Along these lines, the study of the manufacturing technology shows a wide range of textures in the ceramics analysed that could be related to their specific function, while cooking ware (especially cooking plaques) has a coarser texture since a coarser fraction would probably be added, spatulated sherds are finer. XRD and SEM analyses show that most ceramics present a significant dispersion in the equivalent firing temperatures but almost always below 900 °C. Most of them are even lower, having a non-vitrified stage that might give very different mechanical properties than those developed in vitrified stages (Kilikoglou et al., 1995; Kilikoglou et al., 1998; Vekinis and Kilikoglou, 1998; Tite et al., 2001; Hein and Kilikoglou, 2007; Hein et al., 2008). In individual EMP503 (spatulated *sitra*), higher temperatures and a total vitrificated clay matrix have been identified in which the clay matrix shows microbloating pores, suggesting the use of a fast-heating process typically resulting from a bonfire (Buxeda et al. 2003).

5. Conclusions

This study presents for the first time a view regarding the production and distribution of ceramics from the County of Empúries between the 10th and 11th centuries, showing a more dynamic scenario than considered before, thanks to the aid of the analytical examination. The results of the chemical analysis show that the studied set presents a great diversity of productions, with 4 groups related to the County of Empúries and one to the County of Rosselló. Moreover, many individuals remain loners. Most, if not all, seem to be related to a local or regional origin, as confirmed by petrographic analysis and the identification of talc by XRD, suggesting a dispersed production exists. Moreover, some ceramics (CGPGR01 group and loners-PGR) exhibit extremely high sodium concentrations that could be related to pegmatite rocks in the Cap de Creus area.

Besides, at least some of these ceramics were possibly produced in bonfires, and some groups (especially CGEM01 and CGEM02) show a dispersion in the EFT that implies a clear difference in microstructures that would affect their performance characteristics, reflecting a low standardised production.

Nevertheless, there is evidence of the circulation of ceramics over the Albera range, at least for the group of ceramics produced in the County of Rosselló recovered in different sites of the County of Empúries, but not viceversa. That appoints a more significant commercial influence of the northern counties over the southern ones in this period, which should be explored in depth. Along these lines, sharing types, even for the rare cooking plaques produced at both sides of the Albera range, should be interpreted as the existence of common knowledge and ideas between the two areas. Apart from shedding light on possible commercial relationships, this fact demonstrates the importance of craft in culturally connecting the different territories and, at the same time, building political entities such as the medieval Catalan counties, which would be the basis for current Catalonia.

This historical period is very complex because of the fragile political entities and the significant changes that took place. Future research must deepen this problem by trying to study larger samples and more archaeological sites. This research line would help better understand the organisation of these counties in the medieval ages and the construction process of larger national entities.

Credit authorship contribution statement

Marta Valls Llorens: Conceptualization, Data curation, Formal analysis, Investigation, Visualization, Writing – original draft, Writing – review & editing. **Jaume Buxeda i Garrigós:** Conceptualization, Funding acquisition, Investigation, Methodology, Project administration, Resources, Supervision, Validation, Writing – review & editing. **Marisol Madrid i Fernández:** Formal analysis, Investigation, Methodology, Supervision, Validation, Writing – review & editing. **Roberta Bruna Mentesana:** Data curation, Formal analysis, Formal analysis, Validation, Visualization, Writing – review & editing. **Anna Maria Puig Griessenberger:** Funding acquisition, Project administration, Resources, Validation.

Declaration of competing interest

The authors declare that they have no known competing financial interests or personal relationships that could have appeared to influence the work reported in this paper.

Data availability

All data are available in the main document or referenced publications. The WD-XRF and PXRD raw data presented in this study are openly available in the CORA.RDR, Research Data Repository (https://dataverse.csuc.cat/) (Buxeda i Garrigós et al., 2023): 10.34810/data790.

Acknowledgements

We would like to offer special thanks to the Directors of the archaeological sites involved in this project for the cession of the ceramics studied: Joaquim Tremoleda (Sant Martí d'Empúries), Joan Frigola (Torre Lardera), and Olivier Passarrius (Vilarnau and Camp del Rei). X-ray fluorescence, X-ray diffraction and SEM analyses were performed at the Centres Científics i Tecnològics de la Universitat de Barcelona (CCiTUB).

Funding

Marta Valls Llorens is indebted to the Spanish Government (Ministry of Universities) for the predoctoral fellowship within the Formación de Profesorado Universitario program [FPU2018-998758-00791]. Roberta Mentesana performed this research with the grant Juan de la Cierva Incorporación [IJC2020-045094-I] funded by MCIN/AEI [10.13039/501100011033] and by the European Union NextGeneration EU/PRTR funding. This study has been performed in the framework of the project "*Estudi de la caracterització arqueomètrica de ceràmiques d'època carolíngia de Castelló d'Empúries*" (Archaeometric characterisation of the ceramics from the Carolingian period of Castelló d'Empúries), funded by the Institut Ramon Muntaner [AP19/18], Institut d'Estudis Empordanesos and the research unit Cultura Material i Arqueometria of the University of Barcelona (ARQUB, GRACPE) [FBG304419].

Ethics approval and consent

Ethics approval is not applicable. The Directors of all the archaeological sites consent to the use of the ceramics sampled for destructive analyses and the publication of the results.

Appendix A. Supplementary material

Supplementary data to this article can be found online at https://doi.org/10.1016/j.jasrep.2024.104402.

References

Abadal R,d'., 1950. Catalunya carolíngia, 2. Barcelona: Institut d'Estudis Catalans.

Abadal, R.d', 1961. La Pre-Catalunya (segles VIII, IX, X i XI). In: Soldevila, F (ed) Història dels catalans, 2. Barcelona: Ariel.

Aitchison, J., Greenacre, M., 2002. Biplots of compositional data. Appl. Statist. J. r. Stat. Soc. Series C 51, 375–392. https://doi.org/10.1111/1467-9876.00275.

Aitchison, J., 1986. The statistical analysis of compositional data. Monographs on statistics and applied probability. Chapman and Hall, London.

Aquilué, X., Burés, L., 1999. Fase VI: l'època medieval, a Intervencions arqueològiques a Sant Martí d'Empúries (1994-96), in: Aquilué X (ed.) De l'assentament precolonial a l'Empúries actual. Girona: Museu d'Arqueologia de Catalunya, Monografies Emporitanes, 9, pp 423-426.

Beltrán de Heredia Bercero, J., Buxeda i Garrigós, J., Madrid i Fernández, M., Valls Llorens, M., 2018. El taller de Pedralbes i els gresols ceràmics de la Plaça del Rei per la fosa de la plata. Evidències ceràmiques de la Barcelona del segle VIII: arqueologia i arqueometria. Quarhis: Quaderns d'Arqueologia i Història de la Ciutat de Barcelona. 14: 96-121.

Bolòs, J., Hurtado, V., 1998. Atles dels Comtats d'Empúries i Peralada (780-991). Barcelona: Rafel Dalmau Editor.

Bonnassie, P., 1979. Catalunya mil anys enrera,1. Edicions 62, Barcelona.

Borgers, B., Ionescu, C., Gál, A., Neubauer, F., Von Hagke, A.M., Szilagyi, V., Kasztovszky, Z., Gméling, K., Harsányi, I., Barbu-Tudoran, L., 2021. Production technology and knowledge transfer of calcite-tempered grey ware bowls from 2nd-to5th-century CE Noricum (Austria). Archaeometry 65, 480–497. https://doi.org/10.1111/arcm.12823.

Boulvais, P., de Parseval, P., D'Hulst, A., Paris, P., 2006. Carbonate alteration associated with talc-chlorite mineralisation in the eastern Pyrenees, with emphasis on the St. Barthelemy Massif. Mineral. Petrol. 88, 499–526. https://doi.org/10.1007/s00710-006-0124-x.

Boulvais, P., Ruffet, G., Cornichet, J., Mermet, M., 2007. Cretaceous albitisation and dequartzification of Hercynian peraluminous granite in the Salvezines Massif (French Pyrénées). Lithos 93, 89–106. https://doi.org/10.1016/j.lithos.2006.05.001.

Boutin, A., de Saint, B.M., Poujol, M., Boulvais, P., de Parseval, P., Rouleau, C., Robert, J.-F., 2016. Succession of Permian and Mesozoic metasomatic events in the eastern Pyrenees with emphasis on the Trimouns talc–chlorite deposit. Int J Earth Sci (geol Rundsch) 105, 747–770. https://doi.org/10.1007/s00531-015-1223-x.

Buxeda i Garrigós, J., Jones, R.E., Kilikoglou, V., Levi, S.T., Maniatis, Y., Mitchell, J., Vagnetti, L., Wardle, K.A., Andreou, S, 2003. Technology transfer at the periphery of the Mycenaean world: the cases of Mycenaean pottery found in central Macedonia (Greece) and the plain of Sybaris (Italy). Archaeometry. 45: 263–284. 10.1111/1475-4754.00108.

Buxeda i Garrigós, J., Cau Ontiveros, M.A., 2005. Caracterització arqueomètrica de les ceràmiques tardanes de la Plaça del Rei de Barcelona. Quarhis: Quaderns d'Arqueologia i Història de la Ciutat de Barcelona. 1: 91-99.

Buxeda i Garrigós, J., Cau Ontiveros, M.A., 2006. Caracterització arqueomètrica de la ceràmica espatulada de la Plaça del Rei de Barcelona. Quarhis: Quaderns d'Arqueologia i Història de la Ciutat de Barcelona. 2, 140–151.

Buxeda i Garrigós, J., Cau Ontiveros, M.A., 2004. Caracterització arqueomètrica de les produccions tardanes d'Iluro. Laietània. 15, 449–498.

Buxeda i Garrigós, J., Kilikoglou, V., 2003. Total variation as a measure of variability in chemica.l data sets. In: van Zelst, L. (ed), Patterns and process. A Festschrift in Honor of Dr. Edward V. Sayre. Smithsonian Center for Materials Research and Education, Suitland, pp 185–198.

Buxeda i Garrigós, J., Madrid i Fernández, M., 2009. Caracterització arqueomètrica de les ceràmiques de l'Antiguitat Tardana de Santa Margarida (Martorell). Barcelona: Universitat de Barcelona (unpublished research report).

Buxeda i Garrigós, J., Madrid i Fernández, M., 2016a. Designing rigorous research: integrating science and archaeology. In: Hunt A.M.W. (ed) The Oxford Handbook of archaeological ceramic analysis. Oxford University Press, Oxford, pp 19–47.

Buxeda i Garrigós, J., Madrid i Fernández, M., 2016b. Caracterització arqueomètrica de la ceràmica comuna vidriada i de la majòlica. In: Puig, A.M. (coord.), La construcció del Palau del Comte Enric II a Castelló d'Empúries (Alt Empordà). Estudi documental i dels materials arqueològics. Girona: Museu d'Arqueologia de Catalunya-Girona, Sèrie monogràfica, 26, 139–157.

Buxeda i Garrigós, J., Madrid i Fernández, M., Peix, J., Karatasios, I., KIilikoglou, V., 2018. Caracterització arqueomètrica de les ceràmiques i dels morters del jaciment de Puig Rom (Roses). Barcelona: Universitat de Barcelona (unpublished research report).

Buxeda i Garrigós, J., Valls Llorens, M., Madrid i Fernández, M., Mentesana, R.B., 2023. Carolingian pottery from the northeastern Catalan counties, 10.34810/data790, CORA.Repositori de Dades de Recerca, V1, UNF:6:KtQKMovXNtKgwEsM+YTnIQ== [fileUNF].

Buxeda i Garrigós, J., 1999. Alteration and contamination of archaeological ceramics: the perturbation problem. J. Archaeol. Sci. 26:295–313. 10.1006/jasc.1998.0390.

Buxeda i Garrigós, J., 2018. Compositional Data Analysis. In: López Varela, S L (ed). The Encyclopedia of Archaeological Sciences, John Wiley & Sons, Oxford, pp 1–5.

Carreras Planells, J., Losantos, M., Palau Ramírez J Escuer J., 1994a. Mapa Geológico de España, 1:50.000. Hoja 258, Roses. Instituto Tecnológico Geominero de España.

Carreras Planells, J., Palau Ramírez, J., Cirés Fortuny, J., Escuer, J., 1994b. Mapa Geológico de España, 1:50.000. Hoja 221, Portbou. Instituto Tecnológico Geominero de España.

Cingolani, S.M., 2010. Jaume I: Història i mite d'un rei. edicions 62, Barcelona.

Egozcue, J.J., Pawlowsky-Glahn, V., 2011. Basic concepts and procedures. In: Pawlowsky-Glahn V, Buccianti A (eds) Compositional Data Analysis. Theory and Applications, Wiley, Chichester, pp 12–28 10.1002/9781119976462.ch2.

Feliu i Montfort, G., 2007. La presa de Barcelona per Almansor: història i mitificació. Barcelona: Institut d'Estudis Catalans.

Fernández Lara, E., 2021. Caracterización petrográfica y químico-mineralógica de los morteros de Costa de la Serra, Plaça del Rei y Puig-Rom. Master's degree Thesis. Barcelona: Universitat de Barcelona.

Fort i Costa, M., 2006. Geologia del Cap de Creus, Revista de Girona, 236: 69-73.

Frigola, J., Madroñal, A., Valenzuela, A., 2014. Les sitges de l'era d'en Xiua: un exemple de l'alimentació en la Besalú medieval. Quaderns De Les Assemblees D'estudis Sobre El Comtat De Besalú 1, 65–106.

Frigola, J., 2011. La intervenció arqueològica a l'era d'en Xiua (Besalú, la Garrotxa). In: X Assemblea d'estudis sobre el Comtat de Besalú. Besalú, 4 oct 2008. Quaderns de les Assemblees d'Estudis, 10: 151-7.

Gliozzo, E., 2020. Ceramic technology. How to reconstruct the firing process. Archaeol. Anthropol. Sci. 12, 1–24. https://doi.org/10.1007/s12520-020-01132-z.

Greenacre, M., 2010. Biplots in practice. BBVA Foundation Manuals, Fundación BBVA, Bilbao.

Heimann, R.B., Maggetti, M., 2014. Ancient and historical ceramics. Materials, technology, art, and culinary traditions. Schweizerbart Science Publishers, Stuttgart.

Hein, A., Kilikoglou, V., 2007. Modeling of thermal behaviour of ancient metallurgical ceramics. J. Am. Ceram. Soc. 90, 878–884. https://doi.org/10.1111/j.1551-2916.2006.01466.x.

Hein, A., Müller, N.S., Day, P.M., Kilikoglou, V., 2008. Thermal conductivity of archaeological ceramics: the effect of inclusions, porosity and firing temperature. Thermochim Acta 480, 35–42. https://doi.org/10.1016/j.tca.2008.09.012.

Igc Mapa geològic comarcal de Catalunya 1:50.000 2006 Alt Empordà.

IGME, 2008. Mapa Geológico de los Pirineos 1:400.000.

Kilikoglou, V., Vekinis, G., Maniatis, Y., 1995. Toughening of ceramic earthenwares by quartz inclusions: an ancient art revised. Acta Metall. Mater. 43, 2959–2965. https://doi.org/10.1016/0956-7151(95)00006-H.

Kilikoglou, V., Vekinis, G., Maniatis, Y., Day, P., 1998. Mechanical performanceof quartz-tempered ceramics: Part I, strength and toughness. Archaeometry 40, 261–279. https://doi.org/10.1111/j.1475-4754.1998.tb00837.x.

Liu, X., Liu, X., Hu, Y., 2014. Investigation of the thermal decomposition of talc. Clay Clay Miner. 62 (2), 137–144. https://doi.org/10.1346/CCMN.2014.0620206.

Maritan, L., Piovesan, R., Dalconi, M.C., Rius, J., Crespi, A., Vallcorba, O., Casas, L., Vidale, M., Olivieri, L.M., 2018. Looking Like Gold: Chlorite and Talc Transformation in the Golden Slip Ware Production (Swat Valley, North-Western Pakistan), Minerals, 8, 200; 10.3390/min8050200.

Martín-Fernández, J.A., Buxeda i Garrigós, J., Pawlowsky-Glahn, V., 2015. Log ratio Analysis in Archaeometry: Principles and Methods. In: Barceló, J.A., Bogdanovic, I. (eds), Mathematics and Archaeology, CRC Press, Boca Ratón, pp 178-189.

Mata, J.M., 1990. Els minerals de Catalunya. Institut d'Estudis Catalans, Barcelona.

Ollich, I., 1999. Roda: l'Esquerda. "La ciutat carolíngia", in: Catalunya a l'època carolíngia. Art i cultura abans del romànic (segles IX-X). MNAC, Barcelona, pp. 84–88.

Ollich, I., Mataró, M., Puig, A.M., 2018. Santa Creu de Rodes. L'origen i l'evolució del poble medieval i la seva relació amb el territori del Cap de Creus.2014-2018. Memòria de projecte de recerca. Generalitat de Catalunya, Departament de Cultura, Servei d'Arqueologia i Paleontologia.

Passarrius, O., Catafau, A., 2001. L'habitat rural autour de l'an mil. L'exemple du site du Camp del Rey (commune de Baixas, Pyrenées-Orientales). Les Cahiers De Saint-Michel De Cuxà 32, 109–132.

Passarrius, O., Donat, R., Catafau, A., 2008. Vilarnau: un village du Moyen Age en Roussillon. Trabucaire, collection archéologie départamentale, Perpinyà.

Pechar, F., Rykl, D., 1987. Thermal decomposition of natural mordenite. Chem. Pap. 41 (3), 351–362.

Picon, M., 1973. Introduction à l'étude technique des céramiques sigillées de Lezoux. Unversité de Dijon, Dijon.

Poujol, M., Boulvais, P., Kosler, J., 2010. Regional-scale Cretaceous albitisation in the Pyrenees: evidence from in situ U-Th–Pb dating of monazite, titanite and zircon. J. Geol. Soc London 167, 751–767. https://doi.org/10.1144/0016-76492009-144.

Puig Griessenberger, A.M., 1996. La villa Castilione en el territorio Petralatense. La seva topografia urbana i el castell de Castelló. Annals De L'institut D'estudis Empordanesos 29, 47–77.

R Core Team, 2022. R: A language and environment for statistical computing. R Foundation for Statistical Computing, Vienna, Austria. https://www.R-project.org/. Accessed June 1st 2022.

Rendu, C., 2003. La montagne d'Enveig. Un estive pyrénéenne dans la longue durée. Editions Trabucaire, Perpinyà.

Riu, E., 1984. Ceràmica grisa i terrissa popular de la Catalunya medieval. Acta Mediaevalia 2, 29–48.

Roberts, J., 1963. Determination of the firing temperature of ancient ceramics by measurement of thermal expansion. Archaeometry 6, 21–25.

Salrach, J.M., 1993. Bases materials de l'Estat a l'època carolíngia. L'exemple dels comtats catalans. AAVV. Il Es. Jornades De Debat. El Poder De L'estat: Evolució, Força o Raó. Edicions del Centre de Lectura, Reus.

Subías Pascual, E., Puig Griessenberger, A.M., Codina Reina, D., Fiz Fernández, J.I., 2016. El castrum visigòtic de Puig Rom revisitat. Annal De L'institut D'estudis Empordanesos 47, 75–96.

Subías Pascual, E., Puig Griessenberger, A.M., Codina Reina, D., Fiz Fernández, J.I., 2020. El nucli fortificat de Puig Rom i el seu entorn immediat (2014–2017). Tribuna D'arqueologia 2017–2018, 11–34.

Tite, M.S., Maniatis, Y., Meeks, N.D., Bimson, M., Hughes, M.J., Leppard, S.C., 1982. Technological studies of ancient ceramics from the Near East, Aegean and Southeast Europe. In: Wertime, T.A., Wertime, S.F. (Eds.), The Evolution of the First Fire-Using Industries. Smithsonian Institution Press, Washington, pp. 61–71.

Tite, M.S., Kilikoglou, V., Vekinis, G., 2001. Strength, toughness and thermal schock resistance of ancient ceramics, and their influence on technological choice. Archaeometry 43, 301–324. https://doi.org/10.1111/1475-4754.00019.

Valenzuela, A., Madroñal, A., Frigola, J., 2013. Aproximación a la alimentación medieval (ss. XXIII) mediante el análisis faunístico y carpológico. El caso de Besalú (Girona, Catalunya). Revista Arkeogazte 3, 117–135.

van de Boogaart, K.G., Tolosana-Delgado, R., 2013. Analysing compositional data with R. Springer-Verlag, Berlin Heidelberg.

Vekinis, G., Kilikoglou, V., 1998. Mechanical performanceof quartz-tempered ceramics: Part II, Hertzian strength, wear resistence and application to ancient ceramics. Archaeometry 40, 281–292. https://doi.org/10.1111/j.1475-4754.1998.tb00837.x.

Whitbread, I.K., 1989. A Proposal for the Systematic Description of Thin Sections towards the Study of the Ancient Ceramic Technology. In: Maniatis Y (ed.) Archaeometry: Proceedings of the 25th International Symposium (Athens, Greece 1986). Elsevier: Amsterdam, The Netherlands, pp 127–138.

Whitbread I.K., 1995. Appendix III. In Greek Transport Amphorae: A Petrological and Archaeological Study. British School at Athens: London, UK.

Whitbread, I.K., 2016. Fabric Description of Archaeological Ceramics. In: Hunt A (ed.) the Oxford Handbook of Archaeological Ceramic Analysis. Oxford University Press: Oxford, UK, pp 199–216.

Whitney, D.L., Evans, B.W., 2010. Abbreviations for names of rock-forming minerals. Am. Min. 95, 185–187. https://doi.org/10.2138/am.2010.3371.